RESULTS OF INVESTIGATIONS OF THE OPTICAL AND MICROSTRUCTURAL CHARACTERISTICS OF STRATOSPHERIC AEROSOL USING THE METHOD OF LIDAR MEASUREMENT INVERSION OVER TOMSK IN SUMMER, 1991

B.D. Belan, A.V. El'nikov, V.V. Zuev, V.E. Zuev, E.V. Makienko, and V.N. Marichev

Institute of Atmospheric Optics,
Siberian Branch of the Russian Academy of Sciences, Tomsk
Received March 23, 1992

A layer of intensified aerosol scattering in the lower stratosphere has been found and its dynamics has been studied during the lidar monitoring of the troposphere and stratosphere at the High- Altitude Sounding Station of the Institute of Atmospheric Optics in Tomsk in July, 1991. The synoptic situation accompanying the layer appearance has been analyzed. The particle size distribution function, particle number density in the layer under study, and the aerosol scattering coefficients in the spectral interval 0.3–0.7 μm *have been found using the method of inverse problem based on the measurements of the aerosol backscattering coefficient at the wavelengths of* 0.353 *and* 0.532 μm.

Of particular importance in the problem of investigation of the upper atmosphere is the stratospheric aerosol layer at altitudes of from the tropopause to 30 km and its effect on the optical radiation propagation. This interest has primarily been evoked by the observed results which revealed that the average near–ground temperature is a function of the stratospheric aerosol layer transmission for solar radiation. In this context it should be noted that the aerosol particles entering the stratosphere or being directly formed in the stratosphere from gases as a result of chemical and photochemical reactions are accumulated above the tropopause, conserved here much longer than in the lower atmosphere, and propagated at much longer distances due to horizontal transport of air masses. The foundation of the numerical prediction of the effects caused by the aerosol occuring in the stratosphere requires first of all the knowledge of the size distribution and physicochemical properties of particles. This information allows the optical characteristics (volume scattering coefficients, scattering phase function, etc.) to be found in the given wavelength range and the microstructural parameters of interest, such as the total particle number density per unit scattering volume or the number density of individual aerosol fractions, to be determined. In the experiment performed as part of the SATOR program in summer, 1991 the altitude profiles of lidar returns were measured with the help of the lidar system whose aerosol channel employed the pulsed lasers: a YAG laser with wavelength $\lambda = 532$ nm and a gas (excimer) laser with frequency conversion on the basis of stimulated Raman scattering on hydrogen with wavelength $\lambda = 353$ nm. An optoelectronics of the lidar was described in detail elsewhere.[1]

The characteristics of laser radiation are listed in Table I. The measurements were carried out in the photon counting regime with 30–min integration time at the wavelength $\lambda = 532$ nm and 15–min integration time at $\lambda = 353$ nm and the 375–m spatial resolution. The random error in measuring the lidar return with such spatiotemporal characteristics was smaller than 10 % at an altitude of 30 km.

TABLE I. Radiation characteristics of the aerosol channel of the lidar.

Measurable parameters	λ, μm	
	353	532
Pulse repetition frequency, Hz	70	3000
Pulsewidth, ns	10	200
Pulse energy, mJ	15	0.3

In the experiment using the method described in Ref. 2, we determined the altitude profiles from the relation

$$R(H, \lambda_i) = (\beta_{\pi a}(H, \lambda_i) + \beta_{\pi m}(H, \lambda_i))/\beta_{\pi m}(H, \lambda_i) , \qquad (1)$$

where $\beta_{\pi a}(H, \lambda_i)$ and $\beta_{\pi m}(H, \lambda_i)$ are the volume coefficients of aerosol and molecular backscattering at the wavelengths λ_i in the layer centered at the altitude H whose length ΔH is determined by the gate pulsewidth. To increase the efficiency of the technique for reconstructing the profiles $R(H)$ associated with the choice of a calibration point within the 20–35 km altitude range, linear smoothing of the signal[3] was used and the measurement data obtained at night were averaged. The experimental results in the form of the ratio $R(H)$ are shown in Fig. 1 where the altitude profile of the air temperature from the data of meteorological stations located in Kolpashevo and Novosibirsk is also shown.

Figure 1 illustrates most vividly the altitudes of the aerosol layer in the stratosphere and spatiotemporal variations of its structure. It can be seen, in particular, from the behavior of $R(H)$ at the wavelength $\lambda = 532$ nm, at which the effect of the molecular component is much weaker, that during the observations a thick aerosol layer was formed at altitudes of from 15 to 16 km attaining the largest thickness on July 9 when the ratio $R(H)$ in the maximum of the layer reached 2.7. It should be noted that since 1975 such a large value of $R(H)$ comparable to the values typical of the disturbed stratosphere just after volcanic eruptions has been first recorded with the lidar over Tomsk. The analysis of the constant–pressure charts

0235-6880/92/06 373-06 $02.00

showed that the appearance of aerosol layers at altitudes of from 15 to 16 km since July 8, 1991 was caused by the evolution and entrainment of a pressure crest of subtropical air to the south of Western Siberia. On July 7, 1991, before the start of the process, there existed a low-pressure region and a polar tropopause in the stratosphere. Starting from July 7 the pressure crest was formed. On July 8 in the troposphere there were still air masses typical of mid–latitudes while in the stratosphere the subtropical air reached Tomsk. At the same time, on July 8, 1991, there appeared two tropopauses (polar and tropical), one above the other, and an aerosol layer below them at altitudes of from 11 to 16 km.

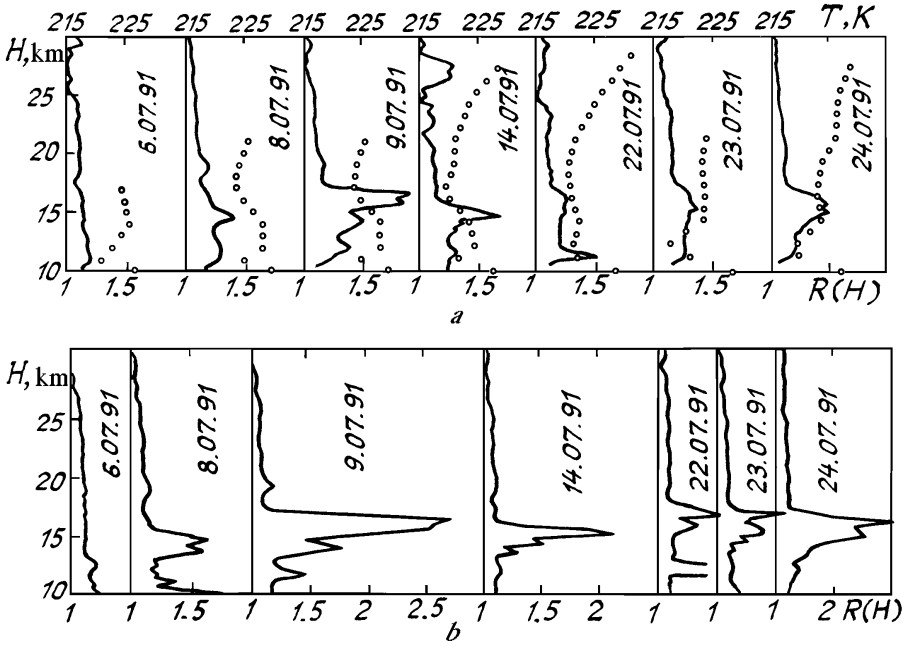

FIG. 1. Vertical profiles of the scattering ratio R(H) measured at the High–Altitude Lidar Sounding Station of the Institute of Atmospheric Optics at the aerosol sounding wavelengths: a) $\lambda = 353$ *and b)* $\lambda = 532$ nm. *Circles denote the air temperature from the data of the meteorological stations located in Kolpashevo and Novosibirsk.*

In analysis of the reasons of aerosol scattering intensification in the lower stratosphere we calculated the trajectory of particle motion in the air mass based on the real wind field at an altitude of 16 km. The calculated trajectory of particle motion denoted by a dashed line in Fig. 2 shows that the formation of the layer with intensified aerosol scattering in the lower stratosphere over Tomsk on July 8 is related to the injection of air mass which on June 25, 1991 was over South–East Asia in the region of Philippine. Taking into account the fact that from June 13 to June 15 the Pinatubo volcano was erupting in Philippine, it is possible to assume that the observed aerosol layer was formed due to aerosol or gas products of volcanic origin entering the stratosphere.

The aerosol particles and volcanic gases injected into the upper atmosphere fell within a jet of the eastern direction located in the 14–30° N latitude belt at the periphery of stratospheric subtropical anticyclones and transported to the south of Western Europe. Over the territory of Western Europe the air flow containing a volcanic plume changed its direction to the southern one and moving in the periphery of the anticyclonic core located here reached a zone of the western flow formed by this core and by a polar cyclone over Ukraine and Belorus (see the scheme in Fig. 2). The pressure crest which entered the south of Western Siberia on July 8 and was located here up to July 15 favored the injection of subtropical air enriched with the products of the volcanic eruption to the region of Tomsk. The intensity of this crest then decreased and the western flows containing the eruption products displaced southerly from Tomsk.

The process under study, including the microstructure and optical properties of stratospheric aerosol, was examined in more detail based on the technique of lidar measurement inversion which was developed, numerically studied as applied to the problems of sounding of the stratospheric aerosol, and tested on the experimental material in Refs. 4 and 5. The initial information for solving the inverse problem incorporated the volume aerosol backscattering coefficients at the sounding wavelengths derived from the profiles $R(H)$ for the values of $\beta_{\pi m}$ calculated with the use of the meteorological data on the vertical profiles of the air pressure and temperature. The measured backscattering coefficients $\beta^*_{\pi i}$, where $i = 1, 2, \ldots, n$, on the assumption of spherical scattering particles, are represented in the form

$$\beta_{\pi i} = \int_{r_1}^{r_2} K_\pi(m, r, \lambda)\, s(r)\, dr\,, \qquad i = 1, 2, \ldots, n, \qquad (2)$$

where $K_\pi(m, r, \lambda)$ is the scattering efficiency calculated according to the formulas of the Mie theory, m is the complex refractive index of particle substance, and $S(r) = \pi r^2 n(r)$, where $n(r)$ is the particle size distribution function defined on the interval of radii $[r_1, r_2]$. System of equations (2) is reduced to the algebraic form

$$\sum_{i=1}^{k} Q_{\pi, il}\, s_l = \beta_{\pi, i}\,, \qquad i = 1, 2, \ldots, n, \qquad (3)$$

in the vector s.

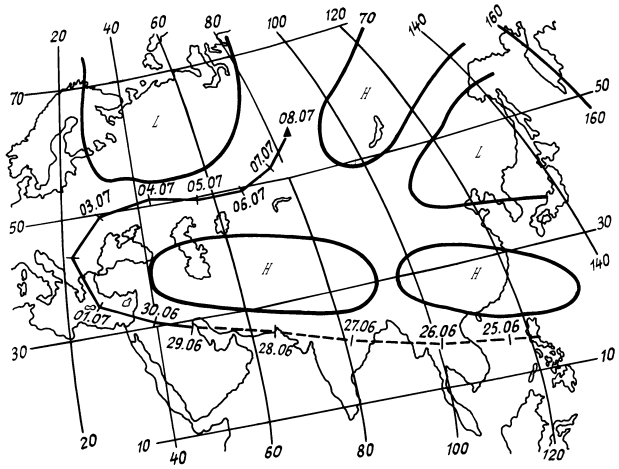

FIG. 2. Synoptic chart during the experiment as part of the SATOR program in July, 1991. The trajectory of particle motion in the air jet (dashed line) was calculated from the observational station (Tomsk).

The vector s^* is taken as a solution of this system which minimizes a quadratic form

$$T_\alpha(s) = \sum_{i=1}^{n}\left(\sum_{l=1}^{k} Q_{\pi,\,il}\, s_l = \beta_{\pi,\,i}\right)^2 + \alpha p \sum_{l=1}^{k-1}(s_{l+1} - s_l)^2 \quad (4)$$

on a set of vectors ψ^+ which is characterized by positive components of any vector belonging to this set, α is the regularization parameter, and p is the weighting factor. The parameter α is chosen consistent with the measurement errors. The obtained vector of solution s^* is employed for reconstructing the examined optical characteristics based on the relations

$$\beta_\pi(\lambda_j) = \sum_{l=1}^{k} Q_{\pi,\,jl}\, s_l^* \,, \; j = 1, 2, \ldots, q, \quad (5)$$

$$\beta_{sc}(\lambda_j) = \sum_{l=1}^{k} Q_{sc,\,jl}\, s_l^* \,.$$

The wavelengths λ_j in Eqs. (5) can lie within the range of sounding Λ or outside it. In this case, the error in reconstructing the optical characteristics increases most markedly as the wavelength λ_j is shifted from the right end of the interval Λ toward the IR region. In the numerical experiment we estimated the information content of the lidar at the given wavelengths.

Because of the small number of wavelengths and, consequently, small dimensionality of the solution the reconstructed distribution functions $s^*(r)$ were very smoothed and characterized the aerosol microstructure on the average rather than yielded information about the details of the particle size spectrum. Moreover, the solution is also smoothed due to the choice of the regularization parameter because of the large error in the initial data at the wavelength $\lambda = 0.353$ μm, in the first place, where the error in determining $\beta^*_{\pi a}(\lambda)$ increases by virtue of the predominant contribution of the molecular component to the lidar return. All these result in the error increase near the maximum and minimum particle radii, in this case, for particle radii < 0.15 μm and > 0.6 μm. In this connection, when determining the particle number density $N(r \geq r_0)$ from the solution $s^*(r)$, we restrict ourselves to the value $r_0 = 0.15$ μm. The measurement error gain in determining $N(r \geq 0.15\ \mu m)$ was ≈ 1.5 while the error in estimating the number of smaller particles sharply increased. It should be noted that more reliable and sufficient for practical applications is the estimate of the total geometric cross sections of particles $S(r \geq r_0)$. However, the estimate of $N(r \geq r_0)$ is most vivid for comparative analysis with the data of direct measurements.

The numerical analysis showed that the errors in reconstructing $\beta_\pi(\lambda)$ in the wavelength range 0.3–0.8 μm are comparable with the errors in measuring $\beta^*_{\pi a}$. It is important to note that the calculational error for this characteristic depended weakly on the errors in the *a priori* choice of the refractive index of the particle substance when the refractive index did not change in the wavelength range. The errors in reconstructing the spectral behavior of $\beta_{sc}(\lambda)$ were larger. When the error of measuring $\beta^*_{\pi a}$ was not larger than 10 %, the error in reconstructing $\beta_{sc}(\lambda)$ in the wavelength range 0.3–0.8 μm was 15–20 % and increased with the wavelength decrease. The most important source of the systematic error in reconstructing the aerosol scattering coefficient based on the aforementioned technique was the *a priori* selection of the particle refractive index. As shown in Ref. 4, the incorrect choice of the real part of the refractive index led to the bias of the calculated optical characteristic from a real one. With deviations $\Delta m = \pm 0.02$ about $m = 1.44$, the corresponding error in determining β_{sc} was at the level of 10–15 %.

When inverting the measurements of $\beta^*_{\pi a}(\lambda)$ we chose the real part of the refractive index $m = 1.43$ and the imaginary one $\kappa = 0$ based on the well–known concepts of aerosol particles under conditions of the "volcanic" stratosphere as droplets of an aqueous solution of sulfurous acid at 75 % concentration of H_2SO_4 and 25 % concentration of H_2O and the optical constants borrowed from Ref. 6. When the percentage of sulfurous acid increased from 70 to 90 %, the values of m, according to the data of Ref. 6, laid in the interval (1.42–1.46).

It can be seen from Fig. 3 that in the course of evolution of the lower stratospheric aerosol layer the particle number density attained its maximum on July 9. Later the particle number density in this layer fell off till July 22. At the same time, this process was accompanied by the increase in the particle number density in the upper aerosol layer at altitudes of from 18 to 22 km from July 9 to July 22 that could testify to the particle transport from the lower aerosol layer to the upper one. On the whole, that process terminated by July 23 when the initial profile of the particle number density observed on July 6 was reproduced in the entire altitude range of the lower stratosphere. Moreover, the particle number density in the upper and, in particular, in the lower aerosol layers on July 6 and July 23 exceeded the background level. The profile for July 6 was possibly not the initial state of the stratospheric aerosol structure but the terminus of a transient process analogous to that observed from July 8 to July 23. As can be seen from Fig. 3, the new stage of this process starts on July 24. Noteworthy is a wide spread of the obtained estimates of the particle number density about the mean values (Fig. 4) which characterizes the stratospheric aerosol instability over the period of observations, especially in the regions between the individual layers at altitudes of 11, 17, and 23 km.

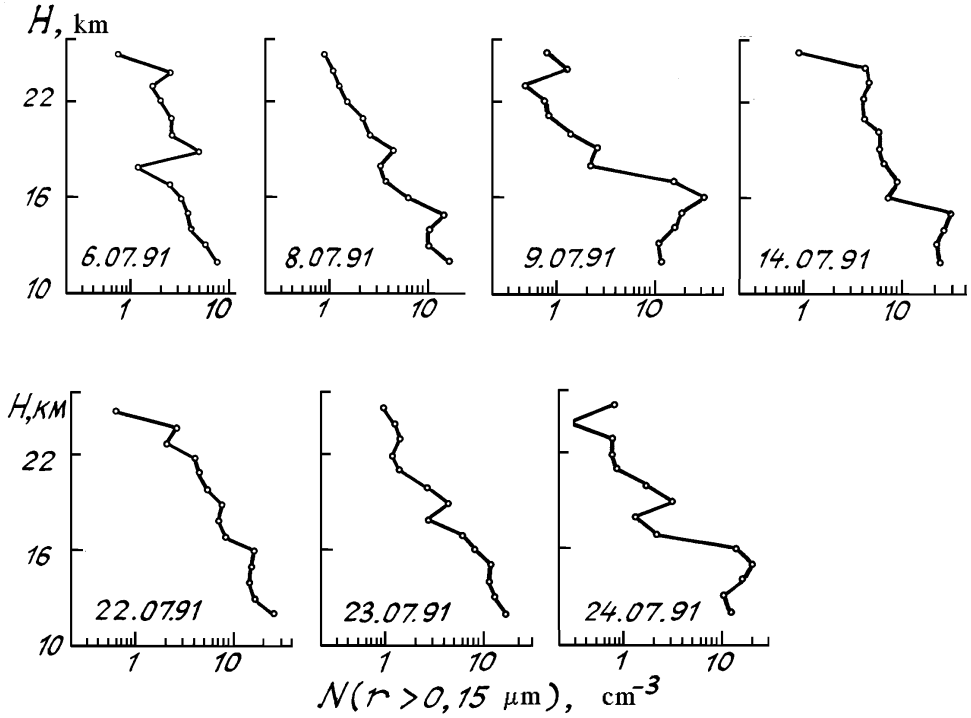

FIG. 3. Spatiotemporal structure of the particle number density from the results of lidar measurement inversion.

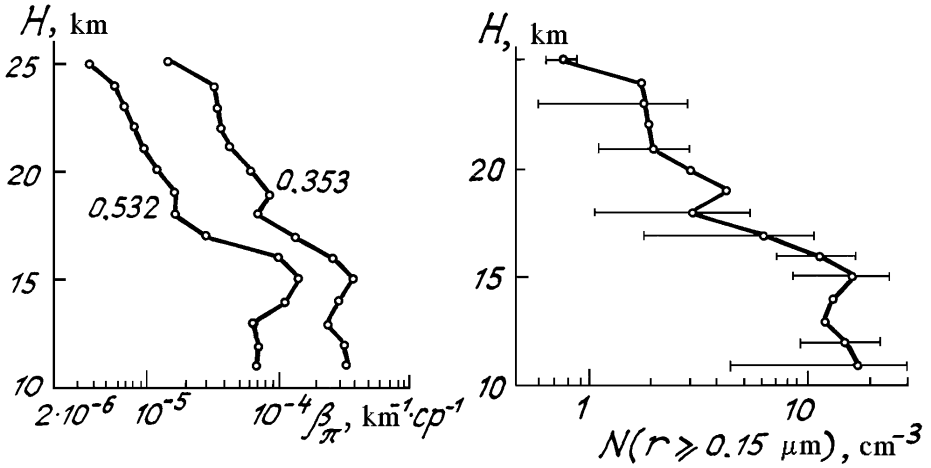

FIG. 4. Vertical profiles of the measured volume aerosol backscattering coefficients (a) and of the particle number density based on the results of experimental data inversion (b) averaged over the period of observation.

The particle size distribution functions derived from the inversion of sounding data and averaged over the period of observations in July, 1991 (Fig. 5) followed the same dependence of $n(r)$ as those reconstructed earlier by the method of inverting the measurements of $\beta^*_{\pi a}(\lambda)$ over Tomsk under conditions of the perturbed stratosphere.[7] This is related to the steepness of the particle size distribution functions $n(r)$ and their localization in the submicron range of the particle size. The same dependence of $n(r)$ was obtained by means of direct measurements at the altitudes below 21 km (see Ref. 8).

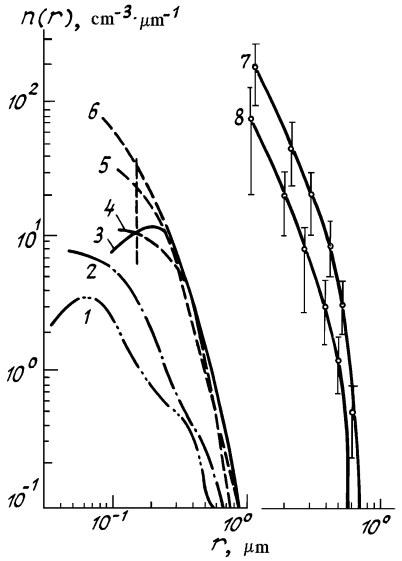

FIG. 5. Examples of the particle size distribution functions borrowed from Ref. 8 (direct measurements) and reconstructed by the inversion of $\beta^*_{\pi a}(\lambda)$: 1) Bigg, Australia, 1969-1974, 2) Bigg, Wyoming, USA,1972, 3, 4, and 5) data for the mid, northern, and tropical latitudes, respectively, borrowed from Ref. 8, 6) results of inversion of the sounding data obtained in Ref. 7 over Tomsk in 1975, 7 and 8) results of inversion of the $\beta^*_{\pi a}(\lambda)$ measurements (over Tomsk in July, 1991 at the wavelengths 0.353 and 0,532 μm averaged over the period of observation. Vertical bars denote the spread of values about the mean (standard deviation).

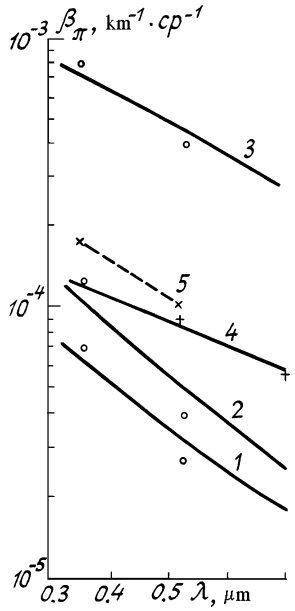

FIG. 6. Spectral behavior of the volume aerosol backscattering coefficients: 1, 2, and 3) $\beta_{\pi\alpha}(\lambda)$ reconstructed by the method of the inverse problem for July 6, 8, and 9, 1991, respectively; 4) results of inversion of the three-frequency sounding data obtained in Ref. 5 over Tomsk in 1975; and, 5) optical–radar model of Ref. 9.

When reconstructing the spectral behavior of the volume aerosol backscattering coefficients (Fig. 6) and volume aerosol scattering coefficients (Fig. 7), we restricted ourselves to the wavelength range 0.308–0.694 μm. Prediction of the optical characteristics at $\lambda = 0.308$ μm has been accomplished to take into account the aerosol contribution at the ozone sounding wavelength. Due to a large volume of experimental data accumulated using a ruby laser lidar, including those obtained over Tomsk, the estimate of optical characteristics at $\lambda = 0.694$ μm is of particular interest for the comparable analysis of long–term observation series. As can be seen from Fig. 6, the absolute values of $\beta^*_{\pi a}(\lambda)$ for July 6 and July 8 and the reconstructed spectral behavior of this characteristic for the same period are typical of the perturbed stratosphere. However, on July 9, 1991 the measurements of $\beta^*_{\pi a}(\lambda)$ exceeded both the model (curve *5* in Fig. 6) and measured values of $\beta^*_{\pi a}(\lambda)$ for July 6, 1991 by several times. At the same time, the spectral behavior of $\beta_{sc}(\lambda)$ for the upper aerosol layer (around 18 km) averaged over the period of observations in July, 1991 is quite similar to McClatchey's model[10] for the same altitude (curves *2* and *4* in Fig. 7) while for the lower aerosol layer (around 16 km) the reconstructed behavior of $\beta_{sc}(\lambda)$ and the model (curve *1* and *3* in Fig. 7) differs strongly in the absolute value. In this case the spread of the estimated values of $\beta_{sc}(\lambda)$ is very wide. The last result shows that the employment of the aerosol model under conditions of such a highly unstable stratosphere can lead to gross errors in accounting for the aerosol effect on one or another process.

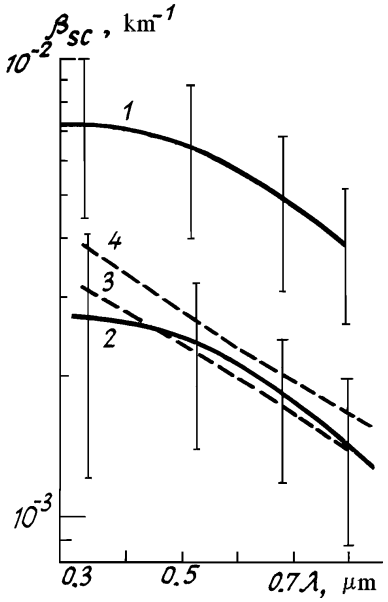

FIG. 7. Spectral behavior of the volume aerosol scattering coefficients $\beta_{sc}(\lambda)$ reconstructed from the inversion of $\beta^*_{\pi a}(\lambda)$: 1) at an altitude of 16 km *and 2) at an altitude of 18 km. Curves 3 and 4 are for the model of Ref. 10 at the same altitudes.*

In conclusion it should be pointed out that to increase the accuracy of interpreting the laser sounding data one needs more accurate data on the particle refractive index. At present, the results of comprehensive studies of the effect of the Pinatubo volcano eruptions and of the composition of aerosol and gas emissions obtained in a large number of research centers are being under processing or publication. The information about the physicochemical properties of aerosol particles entering the stratosphere or being formed as a result of the volcanic gas transformations will make it possible to correct the results of lidar measurement inversion.

REFERENCES

1. A.V. El'nikov, V.N. Marichev, K.D. Shelevoi, and D.I. Shelefontyuk, Opt. Atm. **1**, No. 4, 117–123 (1988).
2. A.V. El'nikov, S.I. Kavkyanov, G.M. Krekov, and V.N. Marichev, Atm. Opt. **2**, No. 5, 438–440 (1989).
3. Yu.V. Chuev, Yu.B. Mikhailov, and V.I. Kuz'min, *Prediction of Quantitative Characteristics and Processes* (Sov. Radio, Moscow, 1975).
4. E.V.Makienko and I.E. Naats, Izv. Akad. Nauk SSSR, Fiz. Atmos. Okeana, No. 9, 991–994 (1983).
5. V.E. Zuev, E.V. Makienko, and I.E. Naats, Dokl. Akad. Nauk SSSR **265**, No. 5, 1105–1108 (1982).
6. K.F. Palmer and D. Williams, Appl. Opt. **14**, 208–219 (1975).
7. E.V. Makienko and I.E. Naats, in: *Study of Atmospheric Aerosol Using the Methods of Laser Sounding* (Nauka, Novosibirsk, 1980), pp. 40–56.
8. N.H. Farlow and G.V. Ferry, J. Geophys. Res. **84**, No. 2, 733–738 (1979).
9. V.M. Orlov, I.V. Samokhvalov, G.M. Krekov, et. al., *Signals and Noise in Laser Sounding* (Radio i Svyaz', Moscow, 1985).
10. R.A. McClatchey, R.W. Fenn, J.E.A. Sebly, et. al., Report AFCRL-71-0279, Bedford (1971).